Study on the Action Mechanism of *Euphorbia peplus* in the Treatment of Alzheimer's Disease Based on UPLC-Q-TOF-MS/MS Combined with Network Pharmacology and Molecular Docking

Liping ZHANG, Weiqing ZHANG, Weixian YANG, Meihui DUAN, Meiqi WEI*

People's Hospital of Anshun City Guizhou Province, Anshun 561000, China

Abstract [**Objectives**] Based on UPLC-Q-TOF-MS/MS, network pharmacology and molecular docking techniques, the mechanism of *Euphorbia peplus* in the treatment of Alzheimer's disease (AD) was studied. [**Methods**] The UPLC-Q-TOF-MS/MS technique was used to rapidly analyze the chemical components of *E. peplus*. Active components and potential targets of *E. peplus* were retrieved from TCMSP and Swiss Target Prediction database, and AD targets were screened using GeneCards database. The targets of *E. peplus* in the treatment of AD were obtained. The PPI network was constructed using String platform, and the network topology of Cytoscape software was used to compute and screen key targets, and the GO and KEGG pathway enrichment analysis was carried out in Metascape database to construct the "component-target-pathway-disease" network. Molecular docking was used to predict the binding properties of active ingredients and targets. [**Results**] The results of UPLC-Q-TOF-MS/MS showed that 83 compounds were identified from *E. peplus*, including 19 terpenoids, 10 phenolic acids and phenols, 16 flavonoids, 2 phenylpropanoids, 4 coumarins, 1 alkaloid, 1 anthraquinone and 30 other compounds. The results of network pharmacological analysis showed that 82 active ingredients were screened, and 279 common targets were identified for the treatment of AD, among which the key targets were ALB (albumin), GAPDH (glyceraldehyde triphosphate dehydrogenase), TNF (tumor necrosis factor), AKT1 (serine/threonine protein kinase 1), and IL6 (interleukin-6). KEGG enrichment analysis showed that key signaling pathways include cancer pathways, lipid and atherosclerosis, Alzheimer's disease, insulin resistance, serotonergic synapses, calcium signaling pathway, cAMP signaling pathway and other signaling pathways. Molecular docking results showed that 14-deoxyandrographolide, dehydroandrographolide, licochalcone B, apigenin and naringenin may be the key components of *E. peplus* in the treatment of AD. [**Conclusions**] The results suggest that *E. peplus* can be used to treat Alzheimer's disease through multi-component, multi-target and multi-pathway.

Key words *Euphorbia peplus*; Alzheimer's disease; Network pharmacology; Molecular docking

DOI:10.19759/j.cnki.2164-4993.2023.04.027

Alzheimer's disease (AD; OMIM: 104300) is the most common neurodegenerative disease in the elderly. Clinically, it shows a continuous deterioration of cognitive and memory function, and progressive decline in daily living ability, accompanied by comprehensive dementia symptoms such as neuropsychiatric symptoms and behavioral disorders. Among them, the vast majority of dementia patients are AD type dementia[1-4]. In recent years, with the aggravation of the aging of the population in China, AD has become the only disease maintaining a rapid growth rate (growth rate > 60%) among all major diseases (tumors, cardiovascular diseases, AIDS)[4-5]. At present, China has the largest number of elderly people and dementia cases in the world[6-7]. Their nursing and treatment will bring a heavy burden to families and society[8-10]. Conducting research on the molecular mechanisms of AD, strengthening understanding of its occurrence and development and finding effective disease prevention, diagnosis and treatment targets are urgent and significant needs.

Euphorbia peplus is a *Euphorbia* plant of the Euphorbiaceae family. *E. peplus* is a temperate annual weed that can grow up to 40 cm tall. It is originally native to Europe and North Africa, but has now become almost cosmopolitan[11-12]. *E. peplus* has strong anti-tumor, cytotoxic, anti-inflammatory and other biological activity[13]. Ingenol compounds are macrocyclic diterpenoid compounds with a 5-7-7-3 ring system found in plants of *Euphorbia* in Euphorbiaceae. They have received widespread attention due to their significant biological activity. In the previous research work, another type of PKC agonists, ingenane compounds discovered from *E. peplus*: C20-deoxyingenol and its derivatives, such as HEP14, can promote lysosomal formation[14]. Subsequent cell-level preliminary screening and mouse model validation showed that this type of compounds can effectively eliminate Aβ (protein aggregates in the brain of elderly dementia patients), with a clearance rate of 32% in mice[14]. These compounds not only activate the autophagy-lysosome system, but also reduce the expression level of AD-related pathway proteins, including BACE1, PSEN1, and PSEN2. This result further confirms that 20-deoxyingenol ester compounds can serve as active lead compounds and have the potential to be developed as a drug for the treatment of neurodegenerative diseases.

Although mouse models have confirmed that this type of compounds has great potential in the treatment of Alzheimer's disease, the number and types of compounds obtained are limited, and comprehensive structure-activity relationship studies have not been conducted, which seriously hinders the further development and utilization of this type of plant. Therefore, based on liquid chromatography-mass spectrometry (LC-MS) combined with network pharmacology and molecular docking techniques, the active

Received: June 3, 2023 Accepted: August 5, 2023

Supported by Science and Technology Fund of the Health Commission of Guizhou Province (gzwkj2021-440).

Liping ZHANG (1990-), female, P. R. China, major: pharmacology.

* Corresponding author.

components of *E. peplus* were rapidly analyzed, and its active targets and mechanism for treating Alzheimer's disease were analyzed and predicted. The exploration on the pharmacologic material basis of *E. peplus* provides reference for its quality control.

Materials and Methods

Materials

Instruments: Dionex Ultimate 3000 RSLC (HPG): Thermo Fisher Scientific; Thermo Scientific Q Exactive Focus: Thermo Scientific Q Exactive Focus; HESI-II: Thermo Fisher Scientific; ACE Ultracore2.5 SuperC18: 100 mm × 2.1 mm.

Reagents: 95% ethanol, methanol, acetonitrile.

Medicinal material: *E. peplus* in Euphorbiaceae.

Methods

Sample treatment and instrument conditions Sample treatment: First, 50 mg of *E. peplus* was extracted by refluxing with 10 times of 95% ethanol for 3 times, 3 h each time, and the extracts were combined. After filtration, the filtrate was concentrated under reduced pressure to recover ethanol and obtain a thick paste. Next, 10 mg of the sample was dissolved in 70% methanol water, and filtered through a 0.22 μm organic microporous filter membrane to obtain a sample of *E. peplus*.

Chromatographic conditions: ACE Ultracore2.5 SuperC18: 100 mm × 2.1 mm; mobile phase: acetonitrile (0.1% formic acid)-0.1% formic acid water; gradient elution; volume flow rate: 0.3 ml/min; column temperature: 40 ℃.

Mass spectrometry conditions: HESI-II ion source; ion source voltage: 3.0 kV (+)/2.5 kV (−); capillary heating temperature: 320 ℃; sheath gas flow rate: 35 arb; auxiliary gas flow rate: 10 arb; ion source temperature: 350 ℃; mass spectrometry scanning method: Full MS ddms2; scanning range: 100 − 1 500 m/z; primary resolution of Full MS: 70 000, and secondary resolution: 17 500.

Data analysis: The data of *E. peplus* were retrieved through the Compound discover software, and the primary and secondary mass spectrometry data of the compounds provided by mass spectrometry scanning were analyzed to identify the compounds. The chemical components of *E. peplus* were determined by screening.

Component collection and active component target prediction of *E. peplus* The 2D structures of the compounds obtained through rapid analysis were saved through Pubchem database[15] (https://pubchem.ncbi.nlm.nih.gov/) in SDF format. The SDF format file was uploaded to Swiss Target Prediction database[16] (http://swisstargetprediction.ch/), and setting the attribute to "Homeo sapiens", prediction analysis was performed through Predict targets to output the information of compound targets. The results were exported and saved in a CSV format file. The chemical component targets were combined using Excel, and targets with "probability ≥ 0" in the predicted results were selected to obtain active component targets. Next, the SDF format file of compounds with high molecular weight or without target acquisition was uploaded to TCMSP[17] (https://old.tcmsp-e.com/tcmsp.php), and an Excel table was obtained. After processing the data, the Uniplot data were uploaded to the Retrieve/ID mapping page of Uniplot[18] (https://www.uniprot.org/id-mapping) to convert UniplotKB AC/ID to gene names. The collected targets were normalized into official names, and the results from the two times of prediction were combined.

Collection of AD-related targets and acquisition of common targets After Logging in to the GeneCards database platform[19], AD-related targets were selected and collected using the search term "Alzheimer's disease", and targets with Relevance scores ≥ 10 were selected in the GeneCards database. The component targets of *E. peplus* and AD-related targets were intersected using Venny (http://www.liuxiaoyuyuan.cn/) to obtain common targets.

Construction of protein-protein interaction network for action targets of *E. peplus* with AD The obtained common targets were imported into the String online platform[20] (https://cn.string-db.org/), and the protein interaction results was obtained by selecting 'Multiple protein', 'Homo Sapiens' for the species, and minimum required interaction score ≥ 0.4. The protein interaction results were downloaded in the TSV format and imported into Cytoscape 3.6.0 software for visual analysis. The CytoNCA plugin was used to calculate the degree, betweenness, and closeness of each target, and the intersection targets with an average of the three ranking in the top 10 were selected as potential key targets.

GO enrichment analysis and KEGG pathway analysis The TSV format file saved in the String database was processed. node1 and node2 were merged, and duplicate values were removed. Next, the data were imported into Metascape database[21] (http://metascape.org/gp/index.html#/main/step1) to conduct GO function and KEGG pathway enrichment analysis. Bioinformatics online platform (http://www.bioinformatics.com.cn/) was used to create visual GO and KEGG diagrams using online drawing tools.

Construction of "*E. peplus* component-AD-target-pathway" network diagram The results were visualized using Cytoscape 3.7.0 software to construct a "component-AD-target-pathway" network diagram. The network diagram obtained was analyzed through the plugin CytoNCA of the software, and an Excel file was exported. The components with high degree values were as screened as key components to conduct molecular docking research.

Molecular docking simulation verification The network topology structures obtained from "Construction of protein-protein interaction network for action targets of *E. peplus* with AD" and "Construction of "*E. peplus* component-AD-target-pathway" network diagram" were analyzed to screen key components and targets. Molecular docking was performed between the obtained components and targets. The 3D structures of key components were downloaded through Pubchem, and the SDF format of the 3D structures was converted into a mol2 format file using OpenBable software. Hydrogens were added through the option of all hydro-

gens, and pdbqt was exported after setting as ligands, detecting and setting twisted bonds. Next, the PDB structures of various targets were downloaded through PDB, and Pymol software was used to delete water and solvent molecules from proteins. Autoduck software was used to add all hydrogens to the structures, which were exported as pdbqt after setting as receptors. Finally, molecular docking was performed using Autoduck software.

Results and Analysis

Main chemical components of *E. peplus*

The samples were processed and detected by the UPLC-Q-TOF-MS/MS technique according to the above method, and chemical components in the ethanol extract of *E. peplus* were qualitatively analyzed. The total ion flow diagram (TLC) of positive and negative ion modes was obtained, as shown in Fig. 1. Based on the compound information generated by mass spectrometry combined with secondary fragment ions and relevant references, qualitative analysis was conducted on the chemical components of *E. peplus*. A total of 83 compounds were identified from *E. peplus*, including 19 terpenoids, 10 phenolic acids and phenols, 16 flavonoids, 2 phenylpropanoids, 4 coumarins, 1 alkaloid, 1 anthraquinone, and 30 other compounds. The molecular formulas, compound names, time, peak areas and other data of the chemical components are shown in Table 1.

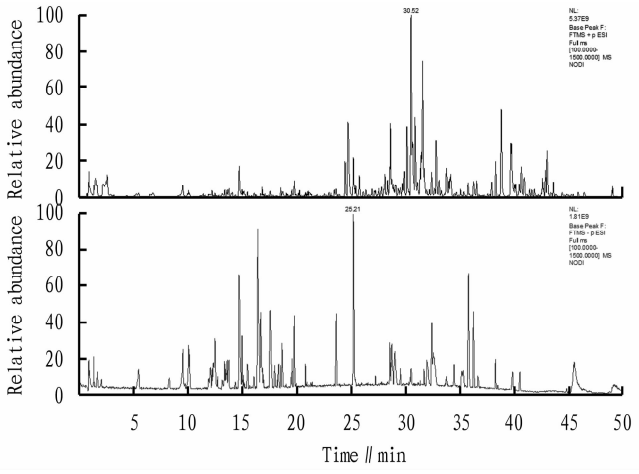

Fig. 1 Total ion flow diagram of *E. peplus* (TLC)

Table 1 Results of composition identification of *E. peplus*

No.	Name	Formula	Molecular weight	RT [min]	Area (Max.)
1	Stachydrine	$C_7H_{13}NO_2$	143.094 39	0.882	120 757 841.7
2	L-Proline	$C_5H_9NO_2$	115.063 43	0.890	36 571 673.25
3	D-Gluconic acid	$C_6H_{12}O_7$	196.057 25	0.890	9 885 253.095
4	L-Valine	$C_5H_{11}NO_2$	117.079 03	1.020	29 622 729.05
5	Ribitol	$C_5H_{12}O_5$	152.067 25	1.040	31 403 594.5
6	Citric acid	$C_6H_8O_7$	192.025 94	1.333	18 177 797.61
7	L-Tyrosine	$C_9H_{11}NO_3$	181.073 66	1.390	11 535 235.16
8	Gamma-Aminobutyric acid	$C_4H_9NO_2$	103.063 52	1.412	435 238.139 7
9	Niacin	$C_6H_5NO_2$	123.032 01	1.424	10 467 203.6
10	Adenosine	$C_{10}H_{13}N_5O_4$	267.096 27	1.476	57 124 701.16
11	Adenine	$C_5H_5N_5$	118.027 75	1.477	16 538 159.57
12	L-Leucine	$C_6H_{13}NO_2$	131.094 39	1.479	104 577 990.8
13	Guanine	$C_5H_5N_5O$	134.022 63	1.561	14 614 664.84
14	Gallate	$C_7H_6O_5$	170.020 36	1.996	36 943 047.17
15	L-Phenylalanine	$C_9H_{11}NO_2$	165.078 69	2.346	56 517 423.73
16	Hydroxytyrosol	$C_8H_{10}O_3$	154.061 84	4.104	103 053.550 4
17	L-tryptophan	$C_{11}H_{12}N_2O_2$	204.089 60	5.221	29 944 181.51
18	Protocatechualdehyde	$C_7H_6O_3$	138.030 41	5.642	4 216 961.975
19	Dacarbazine	$C_6H_{10}N_6O$	182.091 68	5.648	11 007 277.9
20	Trigonelline Hydrochloride	$C_7H_7NO_2$	137.047 52	6.745	32 611 893.77
21	Salicylic acid	$C_7H_6O_3$	138.030 41	6.980	3 504 600.528
22	Gallicin	$C_8H_8O_5$	184.036 16	8.248	37 416 835.52
23	Esculetin	$C_9H_6O_4$	178.025 62	9.273	15 392 247
24	Cryptochlorogenic acid	$C_16H_{18}O_9$	354.094 68	9.501	280 438 381.2
25	Quinic acid	$C_7H_{12}O_6$	192.062 38	9.501	40 803 248.1
26	Caffeic acid	$C_9H_8O_4$	180.041 33	9.952	17 560 122.19
27	Fraxin	$C_{16}H_{18}O_{10}$	370.089 32	10.669	3 963 931.916
28	Isofraxidin	$C_{11}H_{10}O_5$	240.062 87	10.699	2 311 519.378
29	Corilagin	$C_{27}H_{22}O_{18}$	634.079 58	11.209	3 933 564.276

(Continued)

No.	Name	Formula	Molecular weight	RT [min]	Area (Max.)
30	Orientin 2″-O-β-L-galactoside	$C_{27}H_{30}O_{16}$	610.152 49	11.302	11 718 842.91
31	4-Methoxysalicylic acid	$C_8H_8O_4$	168.041 11	12.169	5 568 791.625
32	Bilobalide	$C_{15}H_{18}O_8$	326.099 68	12.198	60 765 443.18
33	Isoschaftoside	$C_{26}H_{28}O_{14}$	564.146 76	12.275	2 896 083.634
34	Vicenin III	$C_{26}H_{28}O_{14}$	564.146 72	12.447	7 078 533.508
35	Phorbol	$C_{20}H_{28}O_6$	364.187 93	12.856	5 465 176.603
36	Scopoletin	$C_{10}H_8O_4$	175.015 43	12.996	4 306 559.136
37	Linderalactone	$C_{15}H_{16}O_3$	244.109 7	13.432	38 677.724 26
38	Gallogen	$C_{14}H_6O_8$	302.005 75	13.458	34 925 701.74
39	Isovitexin	$C_{21}H_{20}O_{10}$	432.104 76	13.511	4 540 187.322
40	Hyperin	$C_{21}H_{20}O_{12}$	464.094 84	13.732	125 711 312.6
41	2'-O-Galloylhyperin	$C_{28}H_{24}O_{16}$	616.105 23	13.852	17 401 122.42
42	Isosakuranetin	$C_{16}H_{14}O_5$	304.094 02	14.449	19 065.207 67
43	Hydroprotopine	$C_{20}H_{19}NO_5$	312.098 86	14.517	1 696 780.233
44	Astragalin	$C_{21}H_{20}O_{11}$	448.099 78	14.692	457 727 279.9
45	Kaempferol	$C_{15}H_{10}O_6$	286.047 14	15.068	19 878 385.85
46	Azelaic acid	$C_9H_{16}O_4$	188.103 73	15.166	11 844 475.36
47 *	Licochalcone B	$C_{16}H_{14}O_5$	286.083 15	15.257	79 344.450 19
48	Ferulic acid	$C_{10}H_{10}O_4$	194.056 76	15.467	39 254 176.23
49	2'-O-Galloylhyperin	$C_{28}H_{24}O_{16}$	616.105 07	15.807	2 411 466.821
50	Noreugenin	$C_{10}H_8O_4$	192.041 75	16.021	6 638 043.114
51	Pennogenin 3-O-β-Chacotrioside	$C_{45}H_{72}O_{17}$	902.485 75	16.547	4 110 443.535
52 *	14-Deoxyandrographolide	$C_{20}H_{30}O_4$	334.213 64	17.064	17 073 760.02
53	Morin	$C_{15}H_{10}O_7$	302.041 91	17.568	46 630 665.48
54	α-Cyperone	$C_{15}H_{22}O$	218.166 54	18.323	2 395 270.483
55	Steviol 19-glucoside	$C_{26}H_{40}O_8$	480.271 43	18.521	51 476 353.07
56 *	Dehydroandrographolide	$C_{20}H_{28}O_4$	332.197 86	18.977	2 122 604.485
57	Neoandrographolide	$C_{26}H_{40}O_8$	480.271 5	19.02	18 121 202.54
58 *	Naringenin	$C_{15}H_{12}O_5$	272.067 86	19.059	3 998 866.726
59 *	Apigenin	$C_{15}H_{10}O_5$	270.052 14	19.243	2 469 101.043
60	Ingenol	$C_{20}H_{28}O_5$	348.192 82	19.548	32 955 508.83
61	Kaempferol	$C_{15}H_{10}O_6$	286.047 08	19.553	61 261 090.13
62	Iristectorigenin B	$C_{17}H_{14}O_7$	330.073 1	19.69	4 713 612.676
63	Spiculisporic acid	$C_{17}H_{28}O_6$	328.187 73	20.264	741 374.274
64	Ailanthone	$C_{20}H_{24}O_7$	376.149 37	20.748	10 501.784 54
65	Croceic acid	$C_{20}H_{24}O_4$	346.177 08	22.347	4 473 412.042
66	Eurycomalactone	$C_{19}H_{24}O_6$	348.154 19	22.429	34 625.16 908
67	Isosteviol	$C_{20}H_{30}O_3$	318.218 67	22.947	22 517 062.73
68	Kahweol	$C_{20}H_{26}O_3$	314.187 52	26.586	5 792 167.836
69	Emodin	$C_{15}H_{10}O_5$	270.052 23	26.623	3 604 471.615
70	Sclareolide	$C_{16}H_{26}O_2$	250.192 62	26.835	2 225 399.522
71	Arenobufagin	$C_{24}H_{32}O_6$	416.218 97	26.917	15 135 721.93
72	Methyl Hexadecanoate	$C_{17}H_{34}O_2$	316.260 66	28.672	36 589 433.64
73	Ingenol-3-angelate	$C_{25}H_{34}O_6$	430.234 67	29.724	70 428 478.11
74	Docetaxel	$C_{43}H_{53}NO_{14}$	807.346 2	31.053	86 417 862.96
75	1-Linoleoyl glycerol	$C_{21}H_{38}O_4$	354.276 07	36.124	7 066 448.594
76	α-Linolenic acid	$C_{18}H_{30}O_2$	278.224 05	36.497	18 344 749.77
77	α-Boswellic acid)	$C_{30}H_{48}O_3$	474.369 98	37.205	10 179 786.12
78	Ursolic acid	$C_{30}H_{48}O_3$	456.359 48	37.497	1 237 071.105
79	Palmitic acid	$C_{16}H_{32}O_2$	256.239 81	39.849	26 093 263.94
80	Lupenone	$C_{30}H_{48}O$	424.369 76	41.896	38 482 666.43
81	Ginkgolic acid GA15∶1	$C_{22}H_{34}O_3$	346.250 21	41.96	1 601 292.106
82	Roburic acid	$C_{30}H_{48}O_2$	440.365 01	42.48	16 901 239.79
83	Ginkgolic acidC17-1	$C_{24}H_{38}O_3$	374.281 42	44.486	5 131 359.454

The key components are marked with *.

Prediction of active component targets in *E. peplus* and screening of AD targets

Target prediction of *E. peplus* was performed using TCMSP and SwissTargetPrediction database platform. ND-30 (orientin 2″-O-β-L-galactoside) had no active targets, and a total of 82 active components were obtained. After removing duplicate values from obtained targets, a total of 723 action targets were obtained. After comparing and intersecting with 1 934 AD-related targets collected under "Collection of AD-related targets and acquisition of common targets" using Venny, 279 common targets were obtained from *E. peplus* for treating AD, as shown in Fig. 2.

Protein-protein interaction network diagram of targets from *E. peplus* for treating AD

The PPI network diagram of the common targets from *E. peplus* for treating AD, which was constructed through online database String, is shown in Fig. 3. Among the 279 targets, 278 were connected with each other, forming 10 698 kinds of interactions, and the color size of nodes were positively correlated with the degree value. The Excel data acquired from cytoNAC plugin were analyzed, obtaining the average values of degree, Betweenness and Closeness as 38.482, 281.10 and 0.503 8, respectively, and 54 common targets were screened based on the three indexes over the average values, including ALB (albumin), GAPDH (glyceraldehyde-3-phosphate dehydrogenase), TNF (tumor necrosis factor), AKT1 (serine/threonine protein kinase 1), IL6 (interleukin-6), VEGFA (vascular endothelial growth factor A), EGFR (epidermal growth factor receptor), SRC (sarcoma virus protein), CASP3 (caspase-3 elisa), MAPK3 (mitogen-activated protein kinase 3), STAT3 (signal transducer and activator of transcription 3), HSP90AA1 (heat shock protein), ESR1 (estrogen receptor gene), HIF1A (hypoxia-inducible factor 1 subunit), MMP9 (matrix metalloproteinase 9), ERBB2 (Erythrocytic Leukemia Virus Oncogene Homology), MTOR (rapamycin), PPARG (peroxisome proliferators-activated receptorγ), MAPK1 (mitogen-activated protein kinase 1), PTGS2 (prostaglandin-endoperoxide synthase 2). The protein interaction topological analysis of the targets is shown in Table 2.

GO functional annotation and KEGG pathway enrichment analysis

The TSV format file saved in String database was processed, including merging node1 and node2 and removing duplicate values, and 278 gene targets were obtained. The Metascape database was used for GO and KEGG analysis. Screening was conducted under the condition of P Value Cutoff = 0.01, and analyzing from biological process (BP), cellular component (CC) and molecular function (MF) aspects, the top 10 BP, MF, and CC results were selected to draw a visualized bar chart, as shown in Fig. 4. In specific, the pathway enrichment analysis involved 2 583 biological processes (BP), including cell response to nitrogen compound, positive regulation of phosphorylation, protein phosphorylation, response to inorganic substance, cell response to organic cyclic compound, response to xenobiotic stimulus, positive regulation of cell migration, behavior, transmembrane receptor protein tyrosine kinase signaling pathway, regulation of system processes, cell response to chemical stress, response to extracellular stimulus,

Table 2 Key targets and their topological characteristics

No.		Degree	Betweenness	Closeness
1	ALB	174	5 343.682	0.727 034 1
2	GAPDH	167	4 737.841 3	0.713 917 55
3	TNF	163	3 466.403 6	0.706 632 7
4	AKT1	162	3 916.501 2	0.706 632 7
5	IL6	159	3 043.748	0.699 494 96
6	VEGFA	142	2 049.894	0.669 082 1
7	EGFR	135	2 299.764 6	0.656 398 1
8	SRC	132	2 171.271	0.653 301 9
9	CASP3	130	1 489.769 8	0.650 234 76
10	MAPK3	126	1 528.588 3	0.644 186
11	STAT3	119	1 033.691	0.630 979 5
12	HSP90AA1	115	1 294.442 6	0.628 117 9
13	ESR1	110	1 172.841	0.616 926 5
14	HIF1A	106	808.033 9	0.611 479 04
15	MMP9	103	868.456 9	0.603 485 8
16	ERBB2	100	880.183 84	0.602 173 9
17	MTOR	98	727.129	0.604 803 5
18	PPARG	95	1 832.979 6	0.599 567 1
19	MAPK1	93	527.428 5	0.594 420 6
20	PTGS2	91	593.208 7	0.594 420 6
21	CCND1	91	461.012 4	0.59314775
22	TLR4	88	515.015 75	0.589 361 7
23	BCL2L1	85	441.192 78	0.579 497 93
24	ANXA5	85	282.535 46	0.573 498 96
25	APP	81	1 634.798 5	0.580 712 8
26	CXCR4	77	885.164 1	0.573 498 96
27	MAPK14	74	355.976 53	0.571 134 03
28	IL2	73	646.460 7	0.563 008 1
29	RELA	72	341.862 7	0.566 462 16
30	MDM2	70	449.113 4	0.564 154 8
31	KDR	70	307.167	0.565 306 1
32	JAK2	68	286.567 6	0.555 110 2
33	GRB2	67	308.458 65	0.557 344 1
34	PPARA	65	871.977 54	0.554
35	MAPT	65	807.133 9	0.555 110 2
36	AR	65	301.822 36	0.549 603 16
37	GSK3B	64	293.102 08	0.557 344 1
38	ACE	64	742.898 2	0.559 595 94
39	FYN	63	497.127 1	0.555 110 2
40	NR3C1	62	459.499 7	0.552 894 23
41	SNCA	58	633.951 6	0.547 430 8
42	REN	54	578.863 46	0.546 351 1
43	PRKCA	53	418.639 62	0.544 204 3
44	F2	53	697.526 4	0.538 910 5
45	NTRK2	53	478.491 58	0.539 961 04
46	TH	50	559.078 74	0.537 864 1
47	CYP3A4	49	519.585 27	0.535 783 35
48	CDK5	47	469.029 6	0.537 864 1
49	PSEN1	45	364.295 07	0.535 783 35
50	CNR1	41	453.486 15	0.523 629 5
51	NGFR	38	282.276	0.523 629 5
52	GSTP1	38	389.216 52	0.515 828 67
53	DRD2	38	393.915 2	0.512 962 94
54	SLC6A4	38	445.593 26	0.512 962 94

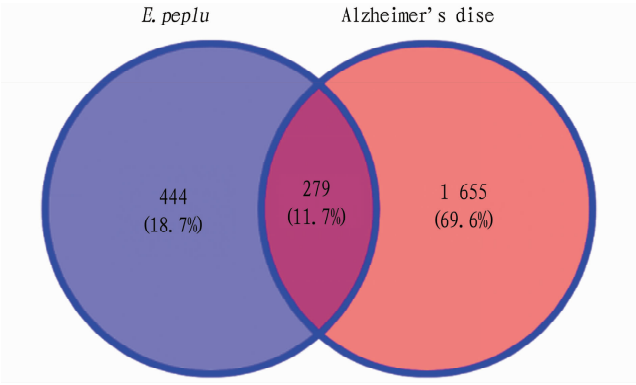

Fig. 2 Common target of *E. peplus* and AD

positive regulation of response to external stimulus, response to salt, response to lipopolysaccharide, secretion regulation, regulation of protein localization establishment, positive regulation of cell death, gland development, and response to wounding. It involved 165 cell components (CC), including membrane raft, dendrite, receptor complex, side of membrane, postsynapse, vesicle lumen, focal adhesion, perinuclear regions of cytoplasm, leading edge of cell, early endosome, extracellular matrix, γ-secretase complex, protein kinase complex, neuromuscular junction, apical part of cell, cytoplasmic side of membrane, organelle outer membrane, endocytic vesicles, nuclear envelope, and platelet α granule. And 293 molecular functions (MF) were involved, including protein kinase activity, protein tyrosine kinase activity, kinase binding, specific binding of protein domain, endopeptidase activity, nuclear receptor activity, phosphatase binding, amide binding, neurotransmitter receptor activity, protein homodimerization activity, heme binding, heat shock protein binding, enzyme activator activity, protease binding, cytokine receptor binding, protein serine/threonine/tyrosine kinase activity, non-membrane spanning protein tyrosine kinase activity, ubiquitin protein ligase binding, ephrin receptor binding, and insulin receptor substrate binding.

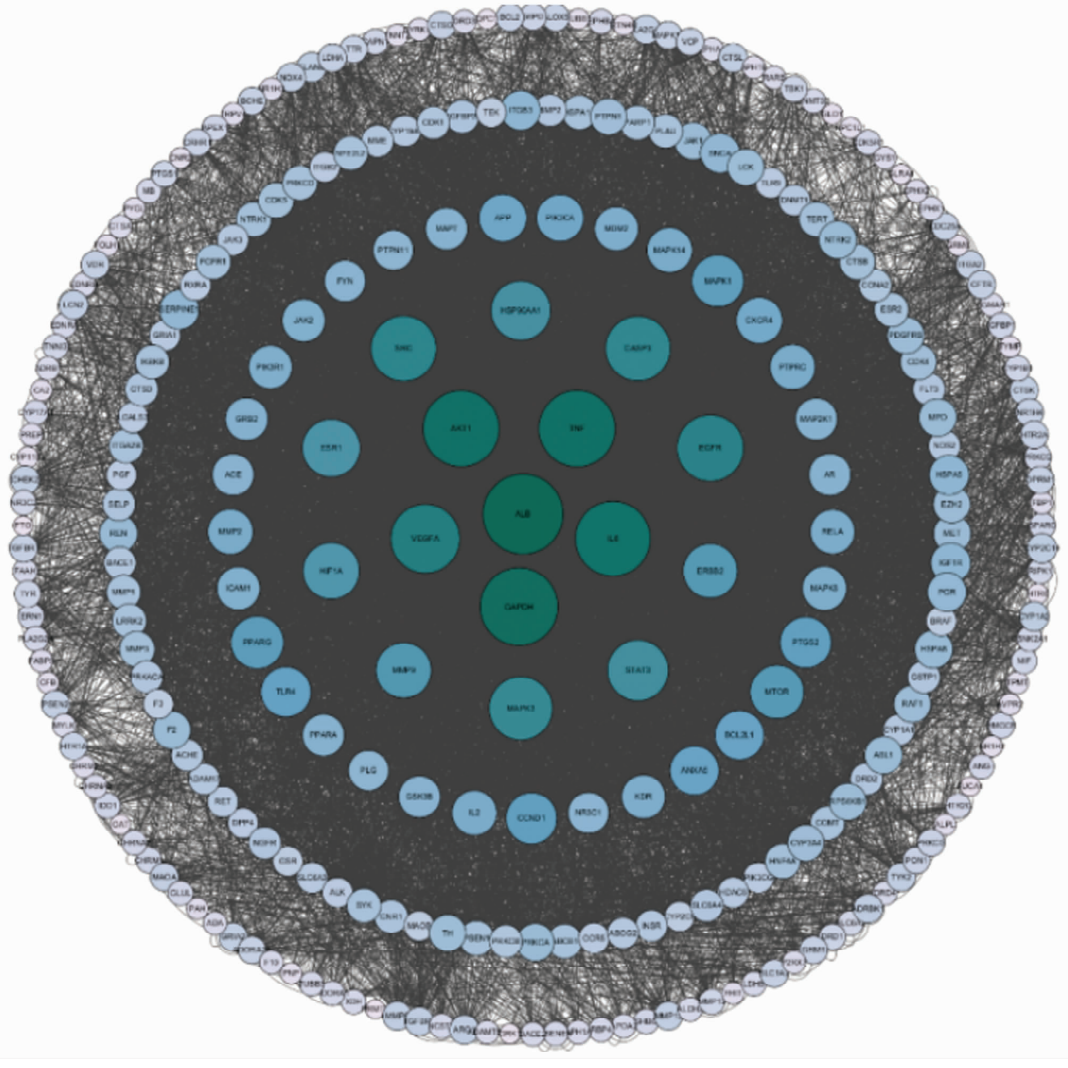

Fig. 3 PPI network diagram

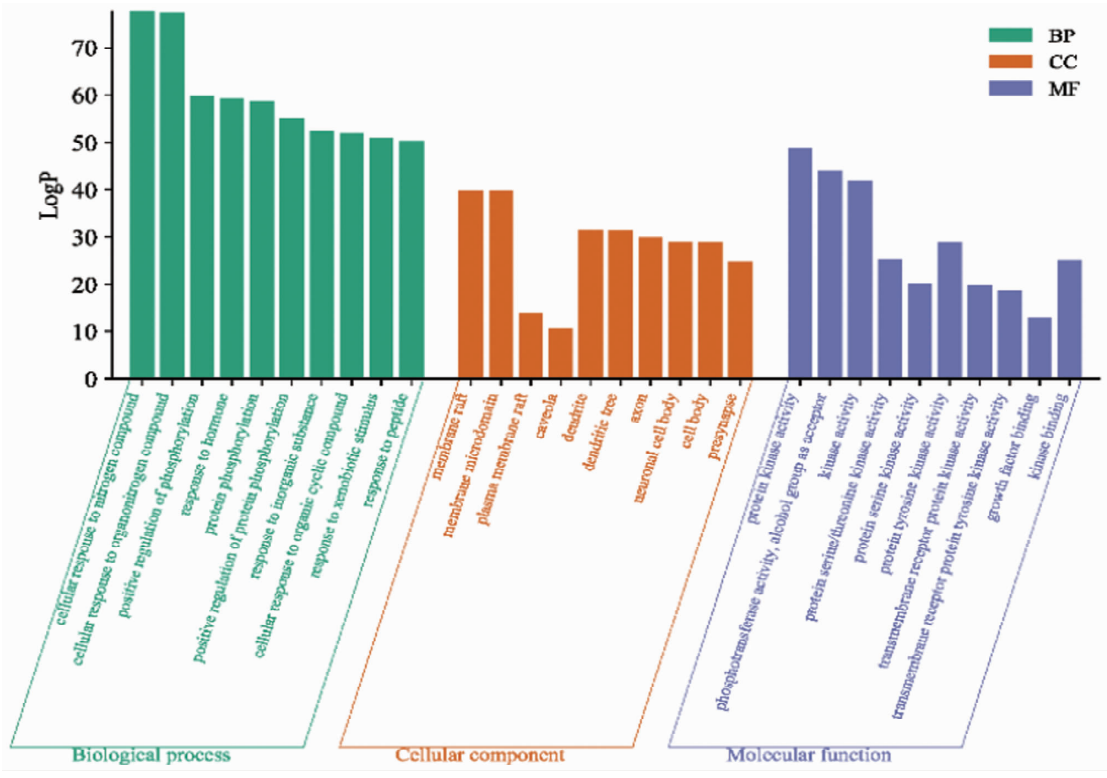

Fig. 4 GO enrichment analysis

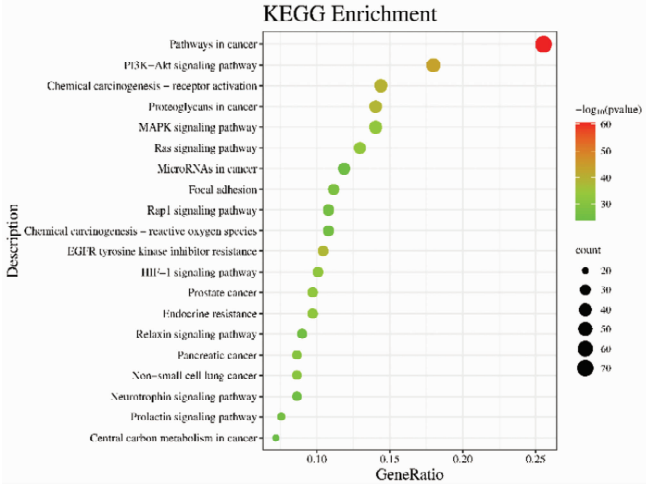

Fig. 5 KEGG and the enrichment analysis

After KEGG enrichment analysis, a total of 222 signal pathways were obtained, and the top 20 items were selected for plot analysis, as shown in Fig. 5. It included not only Alzheimer's disease, and two signal pathways closely related to AD, namely Calcium signaling pathway and cAMP signaling pathway, but also Pathways in cancer, Lipid and atherosclerosis, Insulin resistance, Serotonergic synapse, Bladder cancer, Cholinergic synapse, Dopaminergic synapse, Small cell lung cancer, Inflammatory mediator regulation of TRP channels, NF-κB signaling pathway, Alcoholic liver disease, Transcriptional misregulation in cancer, Amoebiasis, Necroptosis, Adherens junction, AMPK, signaling pathway, Axon guidance, and other signaling pathways.

E. peplus component-AD-target-pathway network diagram

The targets for interaction between *E. peplus* and AD screened by the Cytoscape software were combined with the AD-related pathways obtained through KEGG enrichment analysis to construct a "component-AD-target-pathway" network diagram, as shown in Fig. 6. The network consists of 383 nodes and 2 287 lines, reflecting the pharmacological characteristics of multiple targets and multiple pathways in *E. peplus*. CytoNCA plugin was used to calculate the degree values, and components with degree values ranking in the top 5 were selected as key active components, namely ND52 (14 deoxyandrographolide), ND56 (dehydrated andrographolide), ND47 (licochalcone B), ND59 (apigenin) and ND58 (naringin), as shown in Table 3.

Table 3 Key components and their topological characteristics

	Degree	Betweenness	Closeness
ND52	58	7 693.204	0.410 311 5
ND56	57	7 691.388	0.409 431 93
ND47	55	7 104.699 7	0.407 684 1
ND59	54	3 980.326 4	0.407 684 1
ND58	53	5 608.595 7	0.405 951 1

Molecular docking verification

The molecular docking technique is developed to virtually screen drug targets and predict pharmacological components based on simulating the interaction between ligands and receptors and predicting the binding mode and affinity between protein and protein or small molecule and protein[22]. Molecular docking was performed on key components (ND52, ND56, ND47, ND59, ND58)

of *E. peplus* and key targets (ALB, GAPDH, TNF, AKT1, IL6). It is generally believed that the lower the binding energy of molecular docking, the higher the binding affinity. A binding energy ≤ −4.25 kcal/mol indicates a certain binding activity between the active ingredient and the target; a binding energy ≤ −5.0 kcal/mol indicates good binding activity between the two; and a binding energy ≤ −7.0 kcal/mol indicates strong binding activity between the two. The binding energy between ALB and the key components was less than −7.0 kcal/mol, indicating strong binding activity. The docking results were visualized in Pymol software, as shown in Fig. 7. The molecular docking results showed that the key components and key targets could spontaneously bind, thereby exerting therapeutic effects on AD.

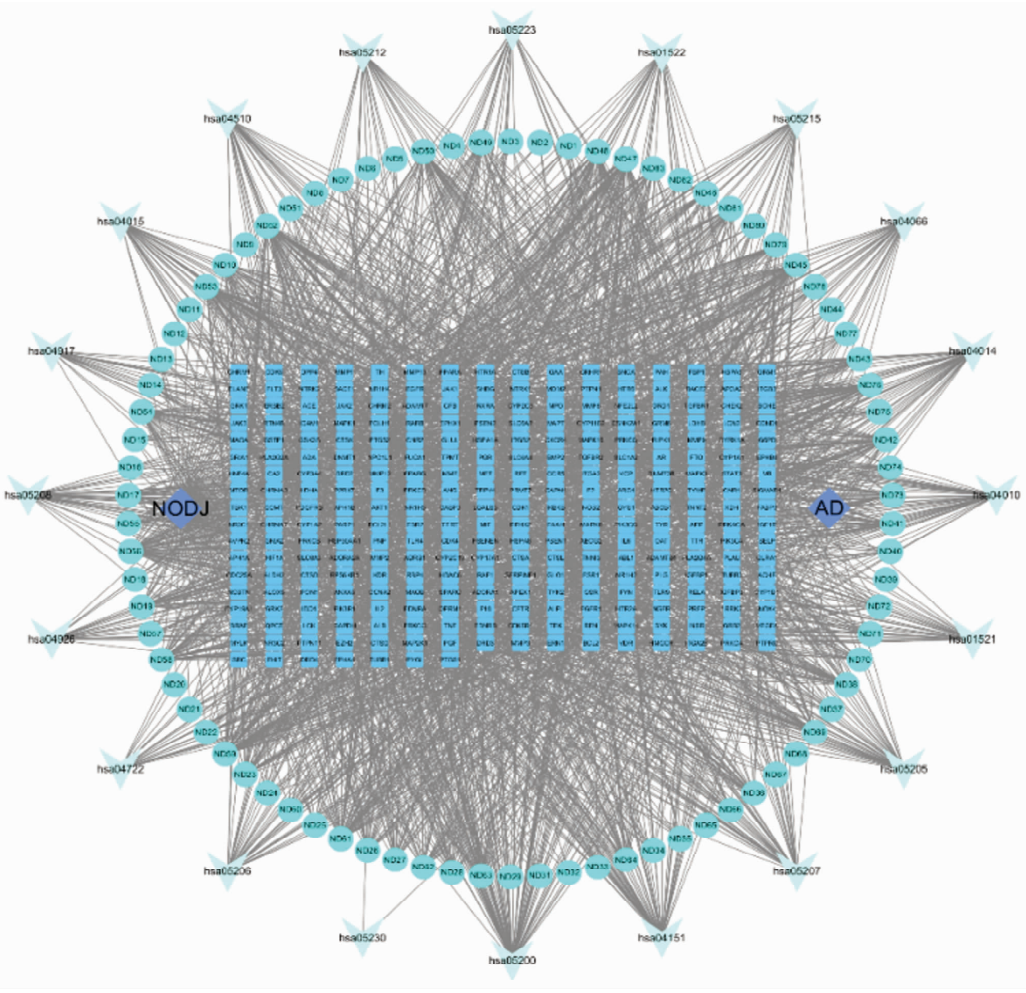

Fig. 6 Component-AD-target-pathway network map

Table 4 Molecular docking data of key components and key targets

	ND52	ND56	ND47	ND59	ND58
ALB	−8.21	−7.43	−7.04	−7.57	−7.77
GAPDH	−5.98	−5.73	−6.04	−5.75	−5.04
TNF	−7.90	−7.32	−6.08	−6.78	−6.11
AKT1	−4.50	−5.19	−4.01	−4.81	−4.20
IL6	−4.52	−5.05	−3.90	−4.48	−3.76

Conclusions and Discussion

In this study, a total of 83 chemical components were quickly analyzed from *E. peplus* by the UPLC-Q-TOF-MS/MS technique, and 60 active components were obtained through TCMSP and Swiss Target Prediction database, and subjected to Venny Diagram analysis with AD targets, which gave 279 common targets. The Excel data obtained from CytoNAC plugin were analyzed, and 54 common targets were identified, including ALB, GAPDH, TNF, AKT1, IL6, VEGFA, EGFR, SRC, CASP3, MAPK3, STAT3, HSP90AA1, ESR1, HIF1A, MMP9, ERBB2, MTOR, PPARG, MAPK1, and PTGS2. The *E. peplus* component-AD-target-pathway-network diagram intuitively showed that multiple active ingredients could exert anti-AD effects through multiple targets and pathways. Meanwhile, ND52 (14 deoxyandrographolide), ND56 (dehydrated andrographolide), ND47 (licochalcone B), ND59 (apigenin) and ND58 (naringin) were screened with high degree values with related targets. The main active components including terpenoids and flavonoids had potential therapeutic effects on Alzheimer's disease in *E. peplus*.

Literature research has shown a correlation between ALB (serum albumin) and Alzheimer's disease[23]. Stanyon *et al.*[24] found that ALB played an important role in regulating the fiber growth of β-amyloid protein in the brain interstitium, thereby affecting the production of AD. The results of research indicated that the ALB of AD patients was lower than that of healthy individuals undergoing physical examination, and the ALB of moderate and severe patients was lower than that of mild patients ($P<0.05$); there was a positive correlation between ALB and MMSE scores in AD patients, while a negative correlation was found between ALB and ADL scores; and it indicated that ALB was closely related to cognitive function[25]. It was found that GAPDH (glyceraldehyde-3-phosphate dehydrogenase) plays a role in non-metabolic processes, such as controlling gene expression and redox posttranslational modifications. Neuroproteomics has revealed a high affinity interaction between GAPDH and Alzheimer's disease protein isolate, and such neuronal protein interaction may lead to damage to the glycolytic function of GAPDH in Alzheimer's disease and may be a precursor to its involvement in cell apoptosis. GAPDH has important significance in the process of neurodegenerative cells, elucidating its role in apoptotic cell death[26]. According to reports, GAPDH interacts with various neurodegenerative disease-related proteins, indicating that GAPDH is a promising therapeutic target for AD[27]. TNF-α plays a crucial role in the pathophysiological process of AD, and the increase in the expression level of TNF-α in AD patients may enhance the production of β-amyloid protein and reduce its degradation, leading to neuronal loss and cell death, as well as cognitive decline in AD patients[28-29]. The results of research found a statistical difference ($P<0.05$) between the Alzheimer's disease group and the control group at the AKT1 gene locus rs2498786, and the AKT1 gene may be a susceptibility gene for Alzheimer's disease and may increase the risk of developing it[30]. From the perspective of target function, IL6 may be the main participant in AD-related immune responses and participate in the progression of neuronal damage during the disease, and the genes encoding IL6 are associated with several diseases and conditions related to inflammation and physiological changes in the human immune system. The genetic association between IL6 and AD supports the importance of immune responses in the occurrence and development of AD[29,31].

In summary, in this study, the action mechanism of *E. peplus* in the treatment of Alzheimer's disease was elucidated through liquid chromatography-mass spectrometry, network pharmacology, and molecular docking methods, fully reflecting the multi-component, multi-target and multi-pathway action mechanism of *E. peplus*, providing a theoretical reference for further elucidating the action mechanism of *E. peplus* in the treatment of Alzheimer's disease. Furthermore, it was found that components such as 14-deoxyandrographolide and dehydrated andrographolide may play an important role in the anti-AD function of *E. peplus*, and further verification is needed.

References

[1] BURNS A, ILIFFE S. Alzheimer's disease[J]. BMJ, 2009, 338: b158.

[2] HUANG Y, MUCKE L. Alzheimer mechanisms and therapeutic strategies [J]. Cell, 2012, 148(6): 1204-1222.

[3] BÄCKMAN L, JONES S, BERGER AK, *et al.* Multiple cognitive deficits during the transition to Alzheimer's disease[J]. J Intern Med, 2004 (256): 195-204.

[4] Alzheimer's Association. 2014 Alzheimer's disease facts and figures[J]. Alzheimers Dement., 2014, 10(2): e47-e92.

[5] Alzheimer's, D. I. World Alzheimer Report 2015[R]. London: Alzheimer's Disease International (ADI), 2015.

[6] JIA J, WANG F, WEI C, *et al.* The prevalence of dementia in urban and rural areas of China[J]. Alzheimers Dement., 2014, 10(1): 1-9.

[7] CHAN KY, WANG W, WU JJ, *et al.* Epidemiology of Alzheimer's disease and other forms of dementia in China, 1990-2010: A systematic review and analysis[J]. Lancet. 2013, 381(9882): 2016-2023.

[8] DOODY RS, RAMAN R, FARLOW M, *et al.* A phase 3 trial of semagacestat for treatment of Alzheimer's disease[J]. N Engl J Med, 2013, 369(4): 341-350.

[9] SALLOWAY S, SPERLING R, FOX NC, *et al.* Two phase 3 trials of bapineuzumab in mild-to-moderate Alzheimer's disease[J]. N Engl J Med., 2014, 370(4): 322-333.

[10] DOODY RS, THOMAS RG, FARLOW M, *et al.* Phase 3 trials of solanezumab for mild-to-moderate Alzheimer's disease[J]. N Engl J Med., 2014, 370(4): 311-321.

[11] OGBOURNE SM, PARSONS PG. The value of nature's natural product library for the discovery of New Chemical Entities: the discovery of ingenol mebutate[J]. Fitoterapia, 2014(98): 36-44.

[12] COREA G, FATTORUSSO C, FATTORUSSO E, *et al.* Amygdaloidins A—L, twelve new 13 α-OH jatrophane diterpenes from *Euphorbia amygdaloides* L.[J]. Tetrahedron, 2005, 61(18): 4485-4494.

[13] VASAS A, HOHMANN J. Euphorbia diterpenes: Isolation, structure, biological activity, and synthesis (2008-2012)[J]. Chemical Reviews, 2014, 114(17): 8579-8612.

[14] LI Y, XU M, DING X, *et al.* Protein kinase C controls lysosome biogenesis independently of mTORC1[J]. Nat. Cell Biol., 2016, 18(10): 1065-1077.

[15] KIM S, CHEN J, CHENG T, *et al.* PubChem in 2021: New data content and improved web interfaces[J]. Nucleic Acids Res., 2021, 49 (D1): D1388-D1395.

[16] GFELLER D, MICHIELIN O, ZOETE V. Shaping the interaction landscape of bioactive molecules[J]. Bioinformatics, 2013, 29(23): 3073-3079.

[17] RU J, LI P, WANG J, *et al.* TCMSP: A database of systems pharmacology for drug discovery from herbal medicines[J]. J Cheminform., 2014 (6): 13.

[18] UniProt Consortium. UniProt: The Universal Protein Knowledgebase in 2023[J]. Nucleic Acids Res., 2023, 51(D1): D523-D531.

[19] RAPPAPORT N, TWIK M, PLASCHKES I, *et al.* MalaCards: An amalgamated human disease compendium with diverse clinical and genetic annotation and structured search[J]. Nucleic Acids Res., 2017, 45 (D1): D877-D887.

[20] SZKLARCZYK D, KIRSCH R, KOUTROULI M, *et al.* The STRING database in 2023: Protein-protein association networks and functional enrichment analyses for any sequenced genome of interest[J]. Nucleic Acids Res. 2023, 51(D1): D638-D646.

[21] ZHOU Y, ZHOU B, PACHE L, *et al.* Metascape provides a biologist-oriented resource for the analysis of systems-level datasets[J]. Nat Commun., 2019, 10(1): 1523.

[22] YAO C, LIN L, WANG M, *et al.* Research on the mechanism of Bagui Tianlong Powder in treating Alzheimer's disease based on bioinformatics, network pharmacology, and molecular docking[J]. Chinese Archives of Traditional Chinese Medicine, 2023, 41(6): 1-5, 259-263.

[23] ZHANG K, QI R. Correlation between serum bilirubin, vitamin B12, serum uric acid, serum albumin and Alzheimer's disease[J]. Medical Journal of Liaoning, 2022, 36(6): 28-30. (in Chinese).

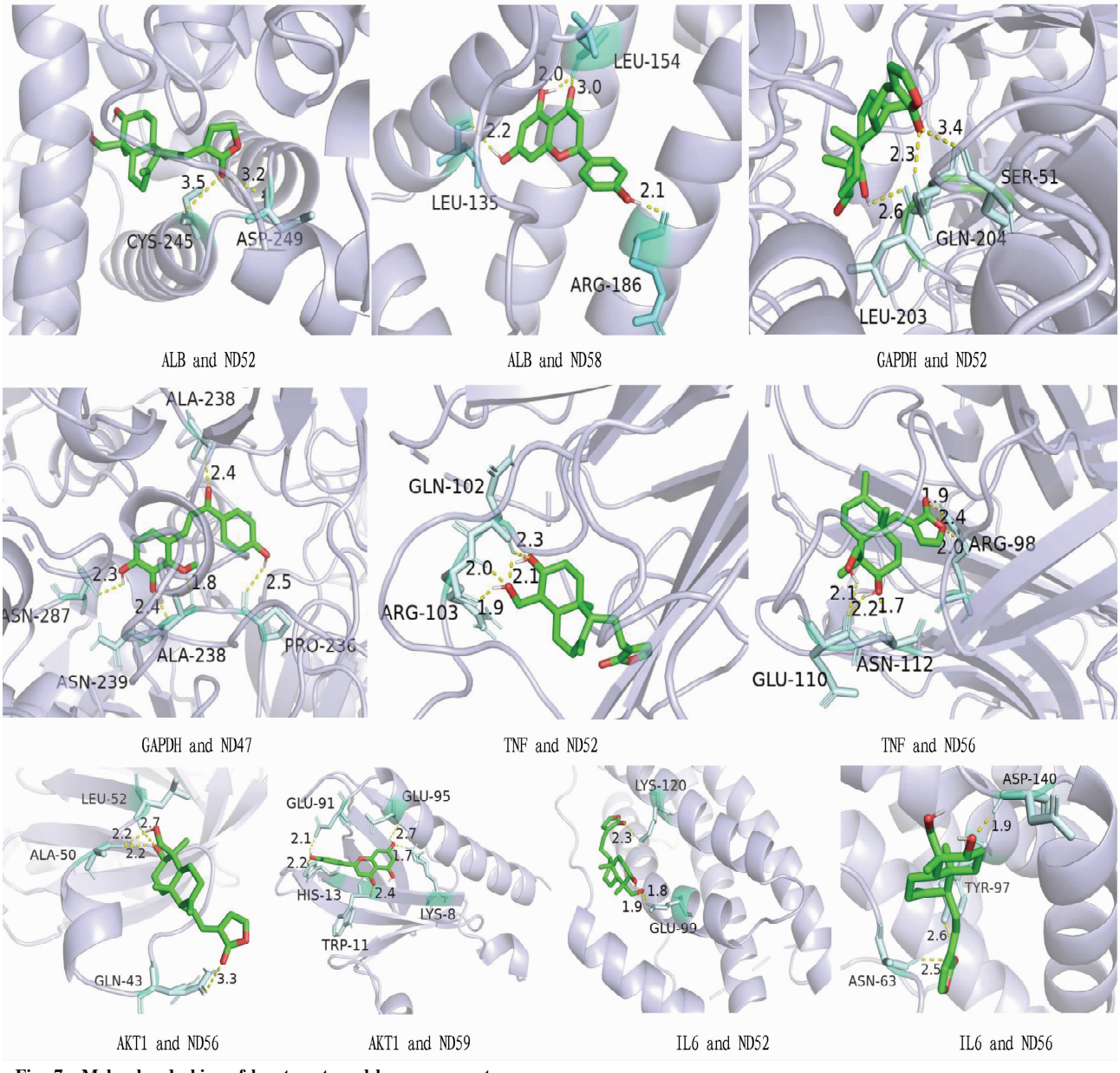

Fig. 7 Molecular docking of key targets and key components

[24] STAYON HF, VILES JH. Human serum albumin can regulate amyloid-β peptide fiber growth in the brain interstitium: Implications for Alzheimer disease[J]. J Biol Chem, 2012, 287(33): 28163 – 28168.

[25] LIU XY, LIU WY, YU XJ, *et al.* Study on correlation between nutritional status and Alzheimer's disease[J]. China Medical Herald, 2014, 11(18): 62 – 65. (in Chinese).

[26] EL KADMIRI N, SLASSI I, EL MOUTAWAKIL B, *et al.* Glyceraldehyde-3-phosphate dehydrogenase (GAPDH) and Alzheimer's disease [J]. Pathol Biol (Paris), 2014, 62(6): 333 – 336.

[27] AHMAD I, SINGH R, PAL S, *et al.* Exploring the role of glycolytic enzymes PFKFB3 and GAPDH in the modulation of Aβ and neurodegeneration and their potential of therapeutic targets in Alzheimer's disease[J]. Appl Biochem Biotechnol., 2023, 195(7):4673 – 4688.

[28] CHANG R, YEE KL, SUMBRIA RK. Tumor necrosis factor α inhibition for Alzheimer's disease [J]. J Cent Nerv Syst Dis., 2017, 9: 1179573517709278. Published 2017 May 15. doi: 10. 1177/1179573517709278.

[29] JIAO ZL, GAO XM. Potential targets and mechanisms of Guarana in the treatment of Alzheimer's disease based on network pharmacology [J]. Digital Chinese Medicine, 2023, 6(1): 55 – 66.

[30] CHEN ZW, ZHAO HD, WANG JL, *et al.* Study on correlation between AKT1 genetic polymorphism and alzheimer disease[J]. China Medicine and Pharmacy, 2016, 6(3): 37 – 40. (in Chinese).

[31] PAPASSOTIROPOULOS A, HOCK C, NITSCH RM. Genetics of interleukin 6: Implications for Alzheimer's disease [J]. Neurobiol Aging, 2001, 22(6): 863 – 871.